

## Electro-optic switching in iron oxide nanoparticle embedded paramagnetic chiral liquid crystal via magneto-electric coupling

Puja Goel, Manju Arora, and Ashok M. Biradar

Citation: [Journal of Applied Physics](#) **115**, 124905 (2014); doi: 10.1063/1.4869740

View online: <http://dx.doi.org/10.1063/1.4869740>

View Table of Contents: <http://scitation.aip.org/content/aip/journal/jap/115/12?ver=pdfcov>

Published by the [AIP Publishing](#)

---

### Articles you may be interested in

[Tuning exchange bias in Fe-/Fe<sub>2</sub>O<sub>3</sub> core-shell nanoparticles: Impacts of interface and surface spins](#)

[Appl. Phys. Lett.](#) **104**, 072407 (2014); 10.1063/1.4865904

[Effect of size, composition, and morphology on magnetic performance: First-order reversal curves evaluation of iron oxide nanoparticles](#)

[J. Appl. Phys.](#) **115**, 044314 (2014); 10.1063/1.4863543

[Influence of excess Fe accumulation over the surface of FePt nanoparticles: Structural and magnetic properties](#)

[J. Appl. Phys.](#) **113**, 134303 (2013); 10.1063/1.4796091

[Preparation of Fe<sub>2</sub>Ni<sub>2</sub>N/SiO<sub>2</sub> nanocomposite via a two-step route and investigation of its electromagnetic properties](#)

[Appl. Phys. Lett.](#) **102**, 012410 (2013); 10.1063/1.4773991

[Magnetic properties of few nanometers -Fe<sub>2</sub>O<sub>3</sub> nanoparticles supported on the silica](#)

[J. Appl. Phys.](#) **111**, 044312 (2012); 10.1063/1.3686647

---



**HIDEN ANALYTICAL** Instruments for Advanced Science

Contact Hiden Analytical for further details:  
[www.HidenAnalytical.com](http://www.HidenAnalytical.com)  
[info@hiden.co.uk](mailto:info@hiden.co.uk)  
**CLICK TO VIEW** our product catalogue

Gas Analysis	Surface Science	Plasma Diagnostics	Vacuum Analysis
 <ul style="list-style-type: none"><li>dynamic measurement of reaction gas streams</li><li>catalysis and thermal analysis</li><li>molecular beam studies</li><li>dissolved species probes</li><li>fermentation, environmental and ecological studies</li></ul>	 <ul style="list-style-type: none"><li>UHV TPD</li><li>SIMS</li><li>end point detection in ion beam etch</li><li>elemental imaging - surface mapping</li></ul>	 <ul style="list-style-type: none"><li>plasma source characterization</li><li>etch and deposition process reaction</li><li>kinetic studies</li><li>analysis of neutral and radical species</li></ul>	 <ul style="list-style-type: none"><li>partial pressure measurement and control of process gases</li><li>reactive sputter process control</li><li>vacuum diagnostics</li><li>vacuum coating process monitoring</li></ul>

## Electro-optic switching in iron oxide nanoparticle embedded paramagnetic chiral liquid crystal via magneto-electric coupling

Puja Goel,<sup>1,a)</sup> Manju Arora,<sup>2</sup> and Ashok M. Biradar<sup>2</sup>

<sup>1</sup>*Division of Agricultural Chemicals, Indian Agricultural Research Institute, New Delhi 110012, India*

<sup>2</sup>*Materials Physics and Engineering Division, CSIR-National Physical Laboratory, Dr. K. S. Krishnan Marg, New Delhi 110012, India*

(Received 14 January 2014; accepted 16 March 2014; published online 27 March 2014)

The variation in optical texture, electro-optic, and dielectric properties of iron oxide nanoparticles (NPs) embedded ferroelectric liquid crystal (FLC) with respect to change in temperature and electrical bias conditions are demonstrated in the current investigations. Improvement in spontaneous polarization and response time in nanocomposites has been attributed to magneto-electric (ME) coupling resulting from the strong interaction among the ferromagnetic nanoparticle's exchange field (due to unpaired  $e^-$ ) and the field of liquid crystal molecular director. Electron paramagnetic resonance spectrum of FLC material gives a broad resonance signal with superimposed components indicating the presence of a source of spin. This paramagnetic behavior of host FLC material had been a major factor in strengthening the guest host interaction by giving an additional possibility of (a) spin-spin interaction and (b) interactions between magnetic-dipole and electric-dipole moments (ME effects) in the composite materials. Furthermore, the phenomenon of dielectric and static memory effect in these composites are also observed which yet again confirms the coupling of magnetic NP's field with FLC's director orientation. We therefore believe that such advanced soft materials holding the optical and electrical properties of conventional LCs with the magnetic and electronic properties of ferromagnetic nanoparticles are going to play a key role in the development of futuristic multifunctional optical devices. © 2014 AIP Publishing LLC.

[<http://dx.doi.org/10.1063/1.4869740>]

### INTRODUCTION

Among all the emerging research wings focusing on Ferroelectric Liquid Crystals (FLCs), one of the latest emerging research areas being the study of composites of FLCs dispersed with magnetic/ferromagnetic nanoparticles (NPs) with an idea of exploring the potential of developing multifunctional FLC based devices. The dielectric and diamagnetic properties of these chiral smectic LCs enable their optical properties to be controlled by applying electric or magnetic fields.<sup>1–15</sup> However, in practice, most liquid crystal based devices so far have been driven by electric fields. Although some early studies suggest the possibility of controlling LC's optical properties by external magnetic field, but generally it cannot be employed due to their feeble sensitivity to magnetic field and very low diamagnetic permeability anisotropy of chiral smectic phases. Therefore, to enhance the functionality of LC based devices, steps are being taken towards developing new magneto-electric (ME) or multi-ferroic (MF) soft materials which can be easily tuned by various external stimuli.<sup>16–18</sup> There are two ways to achieve this: by synthesizing new soft materials (metallomesogens, all-organic chiral radical LCs, etc.) with inherent magneto-electric coupling or by developing composites of two ferroic phases.<sup>19</sup> ME and MF effects of soft materials can be employed to realize magneto- and electro-optic storage devices.

This journey began with the pioneering work of Brochard and de Gennes<sup>20</sup> who, for the first time, coined the term “ferromematics” for referring a mixture of ferromagnetic NPs (FM NPs) and Nematic LCs and theoretically predicted a remarkable enhancement in magnetic field sensitivity of nematic LCs in the presence of low concentrations of FM particles. This fact was later proved experimentally by Chen and Amer<sup>21</sup> in their investigation on “ferromematics” and motivated many successive studies thereon.<sup>22–24</sup> Now, it is not only limited to the FM characteristic of NPs but the size and morphology of NPs have also been found to beautifully engage themselves in tuning the properties of nematic and ferroelectric LC mixtures.<sup>25</sup> For example, Nematic LCs and the chiral nematic LCs could be perfectly aligned in homeotropic and planar geometries by doping a trace of Ni nanospheres and nanobowls owing to the morphology and surface adsorption of FM NPs on underlying substrate. In comparison to Nematic LC, mixtures of FM NPs and ferroelectric LCs which have two fundamental ferroic orders: i.e., ferroelectric and ferromagnetic and thus proves to be more advantageous over ferromematics in terms of recognizing coupling of ferroic orders in constituent phases. In our recent study, we have considered the coupling of strong intrinsic field of Ni NPs with liquid crystal molecular director field to demonstrate a tunable optical memory effect and fast electro-optic response in ferroelectric liquid crystal dispersed with ferromagnetic nickel nanoparticles.<sup>17</sup> In another report, SQUID and calorimetric measurements on mixtures of magnetic iron oxide ( $\text{Fe}_2\text{O}_3$ ) NPs and FLCs

<sup>a)</sup>Author to whom correspondence should be addressed. Electronic mail: [pujagoel@gmail.com](mailto:pujagoel@gmail.com)

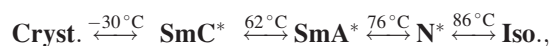
suggested the direct coupling of orientation of magnetic NPs and liquid crystal director field which also affected collective dielectric relaxation processes (Goldstone and Soft Mode) significantly.<sup>13</sup> Recent study on Ni NPs-FLCs composites indicated the occurrence of strong dipole interactions between Ni nanoparticles and FLC molecules in the presence of applied electric field which may lead to improved transmittance and fast switching response.<sup>25</sup> By considering all the previous studies, it can be stated that direct coupling between the orientation of LC molecules and the orientation of magnetic NPs within the host material may lead to the indirect coupling between the ferroic orders thereby resulting into new phenomenon and application potential of soft multi-ferroic materials.

Magnetic NPs of oleic acid coated  $\text{Fe}_2\text{O}_3$  belong to an important class of artificial nanostructured materials for their great potential from application point of view in magnetic storage media and biomedicine as well as fundamental science associated with size driven phenomenon of superparamagnetism, quantum tunneling, and quantum confinement.<sup>26–28</sup> In the present study, we have investigated the mixture of iron oxide NPs ( $\sim 24$  nm) coated with oleic acid surfactant and FLC by temperature-bias dependent dielectric and electro-optic studies. Incorporation of nano-magnetic particles leads to static and dielectric memory effects as well as various interesting changes in physical behavior of composite materials which will be discussed in detail in the present manuscript.

## EXPERIMENTAL

Electro-optic cells for present study consisted of conducting ( $\sim 30 \Omega$ ) indium tin oxide (ITO) coated glass plates with etched squared pattern of  $4.5 \times 4.5$  mm to work as electrode. The patterned and pre aligned (in present case homogenous) substrates were assembled to form a sample cell by placing mylar spacer of known thickness just outside the conducting area. In present case, we have used mylar spacers of  $3 \mu\text{m}$  thickness and the resultant thickness of the empty cells were  $6.6 \mu\text{m}$ . Homogeneous alignment on the patterned glass plates was obtained using conventional rubbed polyimide technique. The FLC-iron oxide NPs composites were fabricated by introducing their mixture into the cells by means of capillary action at temperatures just above the Nematic-Isotropic transition temperature. Suspension of Iron oxide NPs was prepared by dispersing the NPs in oleic acid and deionised (DI) water in ratio of 1:0.5:100 (NPs:oleic acid:DI Water).

First of all, 1 mg of iron oxide NPs and 0.5 mg of oleic acid were mixed in 100 ml water. The resulting solution contains 0.01 mg/ml nanoparticles. Above suspension was ultrasonicated for 1 h before dispersing their selective amount into FLC material.  $0.1 \mu\text{l}$  of this suspension, having 0.000001 mg  $\text{Fe}_2\text{O}_3$  nanoparticles was dispersed in 4 mg FLC, i.e.,  $0.25 \times 10^{-5}$  wt. %. Similarly, other composition of  $0.5 \mu\text{l}$  of NP's suspension was taken in 4 mg FLC ( $1.25 \times 10^{-5}$  wt. %). These mixtures were rigorously mixed and heated repeatedly to ensure homogenous dispersion of NPs among FLC and completely evaporation of solvent. Phase sequence of investigated FLC, i.e., ZLi 3654 is as follows:



where Cryst., SmC\*, SmA\*, N\*, and Iso. represent crystal, chiral smectic C, chiral smectic A, chiral nematic, and isotropic phases respectively. The helical pitch of ZLi 3654 material is  $3.3 \mu\text{m}$ .

To characterize size, morphology, and distribution of iron oxide NPs, High Resolution Transmission Electron Microscopy (HRTEM; Tecnai G2F30 S-Twin) was used. Sample for HRTEM analysis was prepared by dispersing iron oxide NPs in acetone through ultrasonication and drying a droplet of the dispersion on a carbon coated copper grid at room temperature. Optical micrographs of the pure as well as NPs dispersed sample cells were taken with the help of a polarising optical microscope (Ax-40, Carl Zeiss, Göttingen, Germany) fitted with charge coupled device (CCD) camera. The temperature and bias dependent capacitance of sample cells have been measured using an impedance analyser 6540 A (Wayne Kerr electronics, West Sussex, UK) connected with JULABO F-25 HE temperature controller equipment (Julabo, Seelbach, Germany) with a temperature stability of  $\pm 0.01^\circ\text{C}$ . Sample holder containing the sample cells was kept thermally isolated from the external sources. Material parameters, such as spontaneous polarization ( $P_s$ ) and rotational viscosity ( $\eta$ ) with variable electrical bias, were measured by automatic liquid crystal tester (ALCT, Instec, Boulder, CO, USA). Electron Paramagnetic Resonance (EPR) spectrum of FLC mixture ZLi 3645 and  $\text{Fe}_2\text{O}_3$  NPs were recorded by A300 Bruker Biospin, X-band EPR spectrometer at ambient temperature in  $3500 \pm 2500$  G range. Sample is inserted in a transition metal ion free quartz capillary tube of Internal Diameter of 1.00 mm. The sample tubes were placed at the center of circular EPR cavity to exclude asymmetry in resonance signal induced by electric component of the microwave field. DC magnetic field was modulated at 100 kHz frequency and modulation amplitude was kept 6 G to avoid distortion in EPR line shape. Microwave power was also kept very low (23 dB) to avoid any saturation effect. EPR spectrum is generally recorded by scanning the magnetic field (H) at constant microwave frequency (i.e., 9.36 GHz in X-band EPR spectrometer). The position of EPR line depends upon the ratio of H to  $\nu$  and the effective gyrometric factor (g-value). g-value is defined as the constant of proportionality between the frequency and the field at which resonance occurs and proportional to the magnetic moment of the molecule under study. DPPH (1,1-Diphenyl 2-picryl hydrazyl) was used as a standard reference sample for g-value determination.

## RESULTS AND DISCUSSION

In Figure 1(a), TEM micrographs revealed the morphology of iron oxide NPs which are spherical in shape with an average particle diameter of  $\sim 24$  nm and a narrow size distribution. In Figure 1(b), the image of a single particle clearly shows that lattice plane are well aligned and the distance between two lattice planes is about 0.307 nm.

Textural changes caused by dispersing iron oxide NPs into FLC material were checked by recording high resolution optical micrographs of sample cells under a crossed polarizer

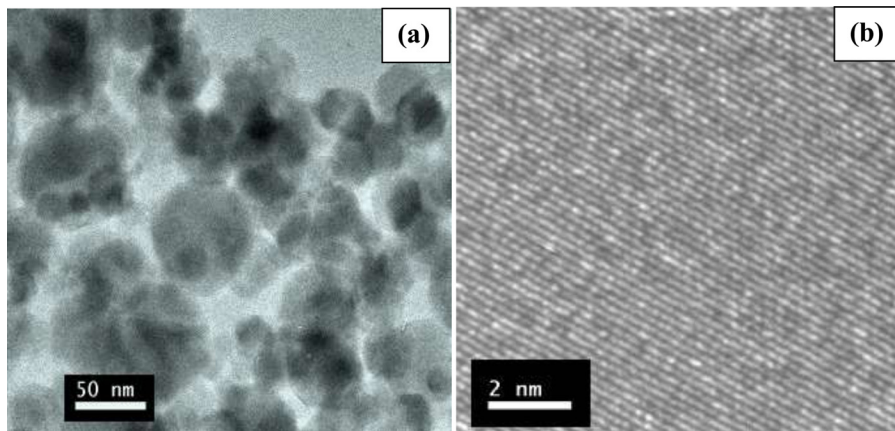


FIG. 1. High resolution transmission electron micrographs. (a) TEM images of the iron oxide NPs (average size of NPs is 24 nm). (b) HRTEM image of NPs.

and it was found that NPs were uniformly dispersed. A close observation reveals strip like domains in iron dispersed samples which might be due to chain like alignment of magnetic NPs within the host material.

EPR spectrum of iron oxide nanoparticles (Fig. 2) shows broad resonance signal with  $g$ -value of 2.0323. The broadness of the signal (peak-to-peak line width ( $\Delta H_{pp}$ )  $\sim$  1000 G) confirms the ferromagnetic behavior of these nanoparticles and strong dipolar-dipolar interactions among them. This resonance signal arises due to  $Fe^{3+}$  in octahedral symmetry. The increase in magnetic crystalline anisotropy and the random orientations of the particles of the monodomain ferromagnetic particles attributes to the strong dipolar-dipolar interaction and broadness of peak.

Behavior of spontaneous polarization on application of electrical bias in ZLi 3654 and iron oxide NPs dispersed samples is compared in Figure 3(a). A gradual enhancement in  $P_s$  can be noted with 0.1 and 0.5  $\mu$ l NPs addition in FLC. Not only this but also the presence of iron oxide NPs makes it easier to get  $P_s$  saturation at lower bias voltages in comparison to pure FLC. For samples containing iron oxide NPs, maximum values of  $P_s$  could be achieved at 5 V, whereas in pure FLC,  $P_s$  saturates at 7.5 V bias. As reported earlier, FM Ni NPs also modified the  $P_s$  values of host material depending on the kind of interaction occurring among the dispersed NPs and

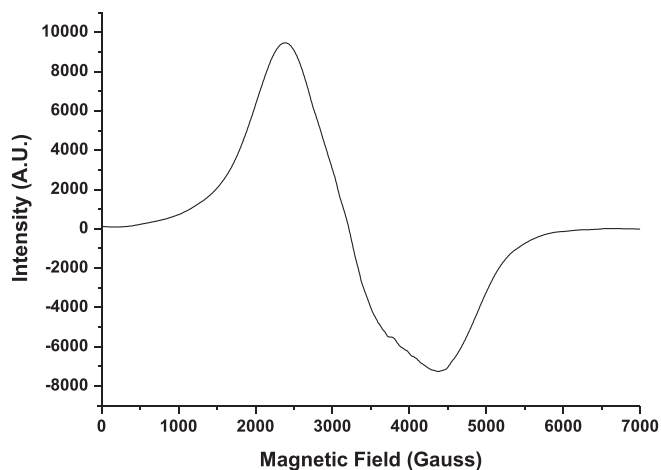


FIG. 2. Broad EPR resonance signal of  $Fe_2O_3$  nanomagnetic particles with  $g$ -value of 2.0322 of  $Fe^{3+}$  ions with octahedral site symmetry exhibiting strong dipolar-dipolar interaction and ferromagnetic behavior.

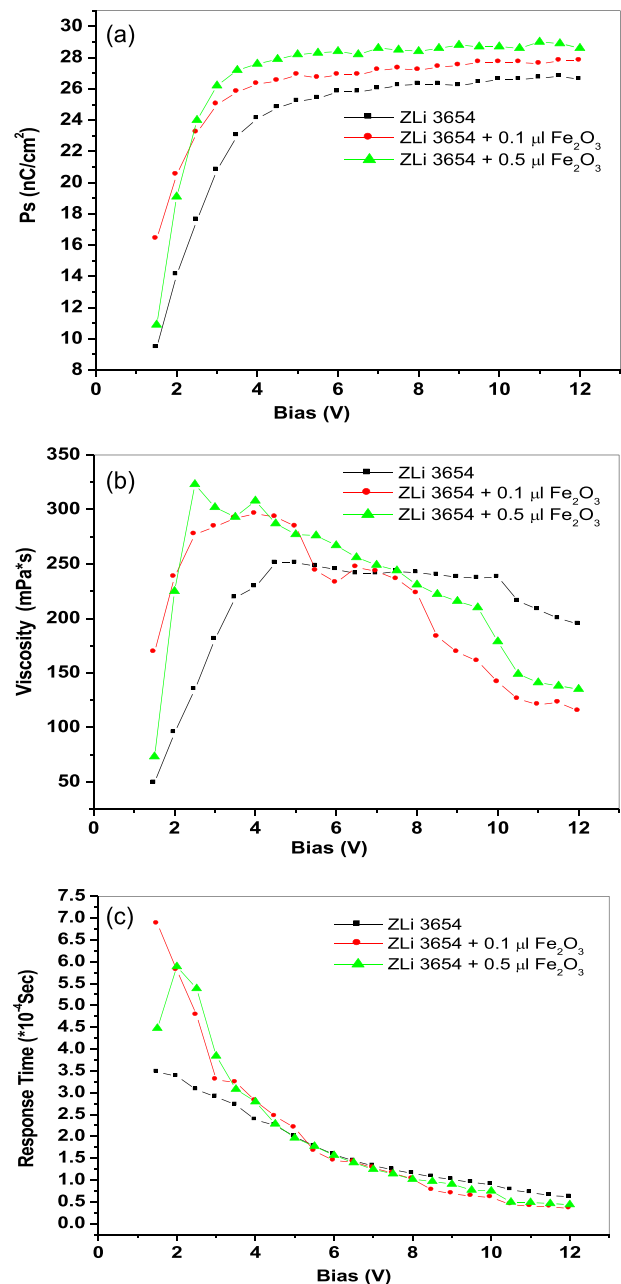
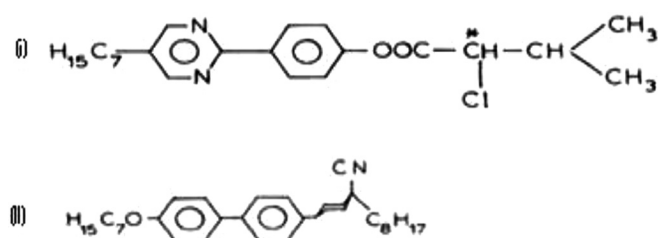


FIG. 3. Electrical Bias dependent behavior of (a) spontaneous polarization ( $P_s$ ), (b) rotational viscosity ( $\eta$ ), and (c) response time ( $\tau$ ) of FLC and FLC-iron oxide NPs dispersions at room temperature.



ferroelectric liquid crystal molecules.<sup>17</sup> Interface bonding mechanism at the FM NPs/ferroelectric LC interface were considered the main mechanism responsible for modifying Ps behavior of samples with low doping concentration of FM NPs whereas exchange interaction dominates in high doping concentrations. In comparison to our previous report on Ni NP doped FLCs, we get a much better profile of Ps along with a decrease in saturation voltage with iron oxide NPs addition, which can be a consequence of the “size effect” phenomenon in FM NPs itself and the chemical constitution of ferroelectric material used. We explained this as follows: If the underlying FLC material is composed of any free radical (unpaired electron), the interaction among the FM NPs exchange field (due to unpaired  $e^-$ ) and FLC molecular director would be much greater than the kind of interaction previously predicted for diamagnetic FLCs in Ref. 24. The FLC mixture used for present study consists of two basic compounds:



In structural formula of compound (i), which is the main chiral component of FLC mixture, there is an asymmetric carbon (indicated by \*) which showed the generation of a sort of spin glass-like inhomogeneous ferromagnetic interactions (the average spin-spin interaction constant  $J > 0$ ) in the bulk liquid crystalline state under weak magnetic fields, has a spin easy axis or exhibits anisotropic magnetic interactions in the  $SmC^*$  phase. This chiral centre is a source of free spin. To establish this, room temperature EPR spectrum of FLC mixture ZLi 3645 is recorded. As shown in Fig. 4, this sample gives a broad resonance signal with superimposed components which may arise from the starred carbon radical. The broadness of the signal is attributed to strong dipolar-dipolar interactions among these spin-glass like FLCs. The

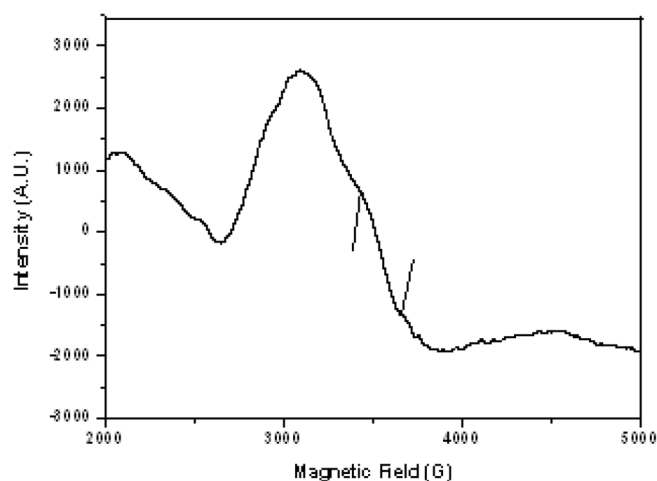


FIG. 4. EPR spectrum of ZLi 3645 mixture in  $SmC^*$  phase with  $g$ -value of 2.0032 submerged in broad asymmetric resonance signal.

$g$ -value of the obtained resonance signal is 2.0036, i.e., close to free electron  $g$ -value (2.0023), which suggests that the resonance comes from the delocalization of the electrons in the  $\pi$ -bonded system of these FLCs via  $-COO$  and  $-CHCl$  chiral group. In this FLC, the starred C atom is chiral centre which is bonded to four different groups. This centre forms a stable free radical by the homolytic fission of either C–H or C–Cl bond facilitated by the delocalization of  $\pi$ -electron of C=O bond of adjacent carboxylic group.

This paramagnetic behavior of host FLC material gives an additional possibility of (a) spin-spin interaction and (b) interactions between magnetic-dipole and electric-dipole moments (ME effects) in the FLC-FM NPs composites.<sup>18</sup> Therefore, it is not only the effect of inter-particle interaction among the dispersed FM NPs but also the direct ME and exchange interaction among LC molecules and FM NPs which in turn strengthens the interfacial bonding between two phases and thereby affects the polarization switching in composite system. Additionally, in iron oxide NPs dispersed FLCs, rotational viscosity (Fig. 3(b)) (i) reaches to maximum around 3 V bias and (ii) continuously decreases thereafter. As a result, response time (which is another vital parameter for display application) of composite material as shown in Fig. 3(c) also decreases with increasing electrical bias above saturation bias voltage. This behavior again indicates that the internal electrical field due to FLC's electrical dipoles is modified in the presence of intrinsic magnetic field of iron oxide particles.

To further analyze the effect of ME coupling and interfacial bonding, textural changes in the iron dispersed samples were recorded in the presence of d.c. bias field. These changes were recorded at different electrical bias conditions using POM and shown in Figs. 5(a)–5(d). Scattered/dark state of the sample ( $0.1 \mu\text{l}$  iron oxide NPs) is shown in Fig. 5(a). Application of 20 V bias across the sample cell brings it to a perfect bright state (Fig. 5(b)) which remains as it is after releasing the bias (Fig. 5(c)). Such static memory

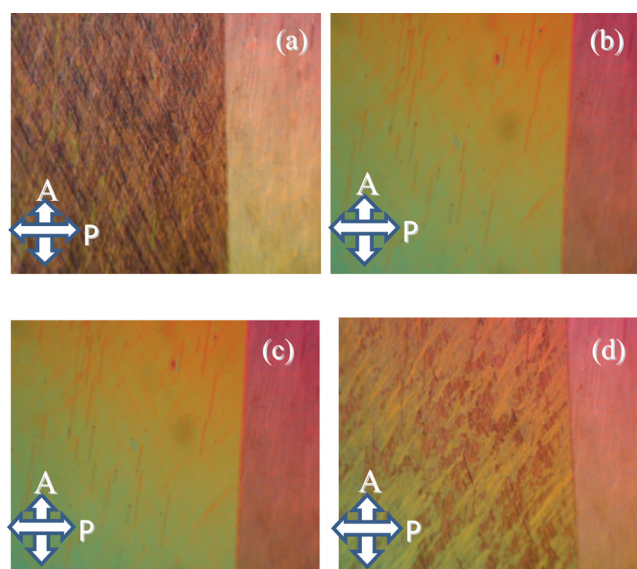


FIG. 5. Room temperature optical micrograph of (a) scattering state before any bias application, (b) completely switched bright state on application of 20 V bias, (c) state after removal of bias, and (d) state after 8 min of bias removal in  $0.1 \mu\text{l}$  iron oxide NPs dispersed FLC mixture.

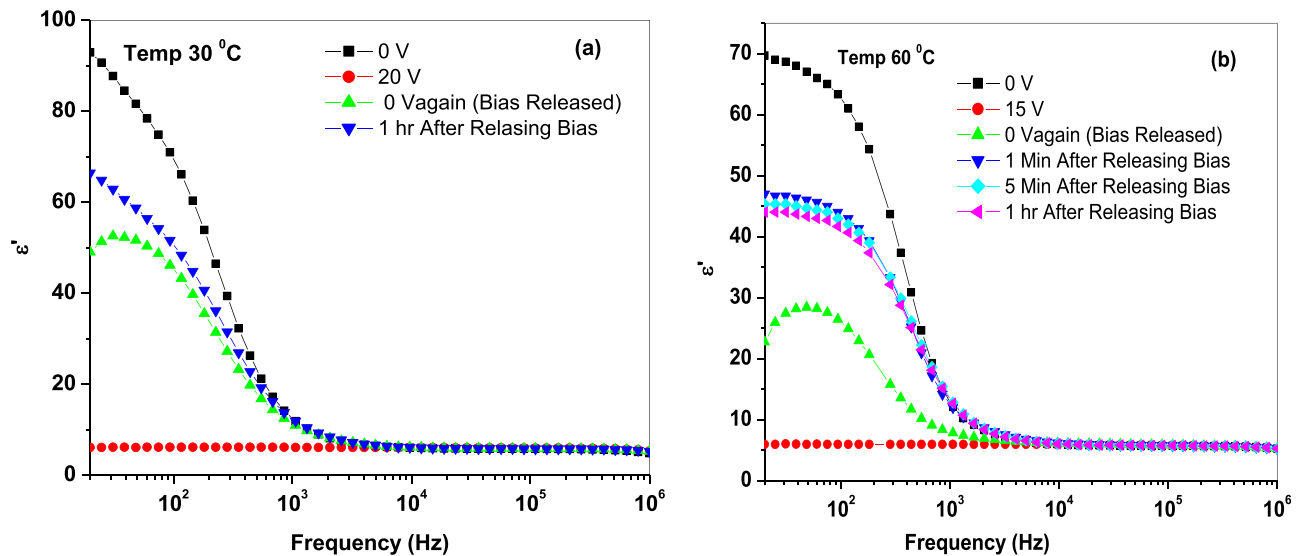


FIG. 6. Frequency-bias-temperature-dependent dielectric permittivity ( $\epsilon'$ ) spectra of  $0.1 \mu\text{l}$  iron oxide NPs mixed FLC sample at (a)  $30^\circ\text{C}$  and (b)  $60^\circ\text{C}$ .

effect was also demonstrated for Ni NPs doped FLCs and explained on the basis of spin dependent screening of electric field in FM/ferroelectric LC mixtures. Memory effects (dielectric and electro-optical) of varied time period have also been reported for gold NPs, ferrofluid, zirconia NPs doped LCs, etc., at different electrical bias, temperature condition. In such mixtures, samples attain their previous state over a certain time period depending on how strongly the depolarizing field is being compensated in the presence of secondary phase nanoparticles. In general, application of appropriate external bias on FLC material causes helix deformation and unwinding which creates a depolarizing field in the direction opposite to induced polarization. In order to minimize the free energy of system, depolarization field works against the changes in material's polarization and forces the molecules back to their previous orientation on the removal of bias. Another factor is the rotational viscosity of the material which can play an important role in relaxing the molecules back to their previous state. A higher viscosity system is more probable to manifest an electro-optic memory state, since it exerts a higher resistance while molecular director changes its orientation. However, in present case, viscosity of system decreases with FM NPs addition, therefore, the observed electro-optic memory state in FLC-FM NPs mixtures cannot be ascribed to the viscosity driven effects. Rather it has been attributed to the strong interaction between FLC molecular director and FM NP's intrinsic magnetic field which modifies the depolarizing field forces which in turn affects the electro-optical states of samples very significantly.

In iron containing samples, complete scattered state was not obtained even after shortening the sample. The optical texture recorded after 8 min of releasing the bias has been shown in Fig. 5(d). There occurs an intermediate state (composed of some dark domains) which is neither perfectly bright nor perfectly dark. This might be due to a change in the orientational distribution of FM NPs among the FLC mixture and formation of magnetic domains in the process of applying and releasing electrical bias. These domains could be

dissociated only on the application of a high frequency low voltage signal or by changing the temperature of samples.

Manifestation of strong interfacial coupling between NPs and FLC molecules can also be seen through the frequency-bias-dependent dielectric permittivity ( $\epsilon'$ ) response of the samples containing iron oxide NPs. As shown in Figure 6(a), the magnitude of  $\epsilon'$  is very large in low frequency range ( $<1 \text{ KHz}$ ) and that is mainly due to the Goldstone mode (phase fluctuations) contribution. Application of 20 V bias suppresses the permittivity to a very low value owing to the suppression of Goldstone mode (deformation and unwinding of helix) which is the main contributor to dielectric permittivity in lower frequency regime. After releasing this electrical bias, sample could attain only 50% of the actual value of dielectric permittivity in iron oxide doped samples. Dielectric permittivity was further recorded after 1 h of releasing the bias, but  $\epsilon'$  value was still much lower than its value in no bias state. This again confirms that the application of d.c. bias changes the orientational ordering of NPs and forces the molecular director to clamp in an intermediate state as demonstrated through the bias dependent optical textures studies. In pure samples also, dielectric permittivity attains its normal value in 50 s after releasing the bias which is due to the relatively higher viscosity of paramagnetic chiral LC material ZLi 3654 in comparison to typical diamagnetic FLCs. Since rotational viscosity of iron oxide dispersed samples shows a decreasing trend with increasing bias, we again believe that effect of ME coupling and strong interfacial bonding is letting the  $\epsilon'$  in a suppressed state even after a long time of releasing the electrical bias. Similar trend of dielectric memory state was confirmed up to the  $\text{Sm C}^* \text{-SmA}^*$  transition temperature of material (Fig. 6(b)), the only difference is that memory state could be observed at a lower bias as the temperature reaches near transition.

## CONCLUSIONS

Current study demonstrates the effect of ME coupling on display parameters as well as electro-optic and dielectric behavior in nanomagnetic iron oxide NPs and ferroelectric

liquid crystal composites. Incorporation of iron oxide NPs makes it easier to get better profile of display parameters, i.e.,  $P_s$  and  $\tau$ , at lower saturation voltages in comparison to pure FLC. The improvement in  $P_s$  and  $\tau$  has been a consequence of the strong interaction among the FM NPs exchange field (due to unpaired  $e^-$ ) and FLC molecular director. It has also been established that the presence of free radical (unpaired electron) in FLC material would strengthen the guest host interaction. EPR spectra of pure FLC mixture showed the generation of a sort of spin glass-like inhomogeneous ferromagnetic interactions (the average spin-spin interaction constant  $J > 0$ ) in the bulk liquid crystalline state under weak magnetic fields which indicated that asymmetric carbon in chiral component of FLC mixture, has a spin easy axis or exhibits anisotropic magnetic interactions in the SmC\* phase. This chiral centre acts a source of free spin and played a role in modifying the internal electrical field due to FLC's electrical dipoles in the presence of intrinsic magnetic field of iron oxide particles. However, these are just preliminary results with their plausible explanation and hence further crucial experiments and simulations are required to probe the exact mechanism behind such magneto-electric coupling. We are pretty sure that these iron oxide NPs mixed FLC nanocomposites are definitely going to play their indispensable role in the production of new generation multifunctional FLCs electro-optical devices.

#### ACKNOWLEDGMENTS

The authors sincerely thank Professor H. S. Gupta, Director, IARI for continuous encouragement and interest in

this work. One of the authors (P.G.) is also thankful to DST, New Delhi for financial support under Project No. SR/WOS-A/PS-68/2011 and INSPIRE Faculty Scheme.

- <sup>1</sup>G. W. Taylor, *Ferroelectric Liquid Crystals—Principles, Preparations and Applications* (Gordon & Breach, New York, 1991).
- <sup>2</sup>P. Kopcansky *et al.*, *Czech. J. Phys.* **51**, 59 (2001).
- <sup>3</sup>Y. D. Gu and N. L. Abbott, *Phys. Rev. Lett.* **85**, 4719 (2000).
- <sup>4</sup>H. S. Kitzerow *et al.*, *Chirality in Liquid Crystals* (Springer, Berlin, Germany, 2001).
- <sup>5</sup>R. Pratibha *et al.*, *J. Appl. Phys.* **107**, 063511 (2010).
- <sup>6</sup>F. V. Podgornov *et al.*, *Appl. Phys. Lett.* **97**, 212903 (2010).
- <sup>7</sup>P. Malik *et al.*, *Adv. Condens. Matter Phys.* **2012**, 853160.
- <sup>8</sup>P. Arora *et al.*, *Mol. Cryst. Liq. Cryst.* **502**, 1 (2009).
- <sup>9</sup>M. K. Paul *et al.*, *Liq. Cryst.* **41**, 635 (2014).
- <sup>10</sup>S. K. Gupta *et al.*, *Curr. Appl. Phys.* **13**, 684 (2013).
- <sup>11</sup>Neeraj and K. K. Raina, *Physica B* **434**, 1 (2014).
- <sup>12</sup>R. Manohar *et al.*, *Polym. Compos.* **31**, 1776 (2010).
- <sup>13</sup>A. Kumar *et al.*, *Appl. Phys. Lett.* **100**, 054102 (2012).
- <sup>14</sup>P. Goel, *RSC Adv.* **4**, 11351 (2014).
- <sup>15</sup>P. Goel *et al.*, *Liq. Cryst.* **39**, 927 (2012).
- <sup>16</sup>B. Rožič *et al.*, *Ferroelectrics* **410**, 37 (2010).
- <sup>17</sup>P. Goel and A. M. Biradar, *Appl. Phys. Lett.* **101**, 074109 (2012).
- <sup>18</sup>R. Tamura *et al.*, *J. Mater. Chem.* **18**, 2872 (2008).
- <sup>19</sup>K. Binnemans, *J. Mater. Chem.* **19**, 448 (2009).
- <sup>20</sup>F. Brochard and P. G. de Gennes, *J. Phys. France* **31**, 691 (1970).
- <sup>21</sup>S.-H. Chen and N. M. Amer, *Phys. Rev. Lett.* **51**, 2298 (1983).
- <sup>22</sup>B. Kinkead and T. Hegmann, *J. Mater. Chem.* **20**, 448 (2010).
- <sup>23</sup>W. Zhou *et al.*, *J. Am. Chem. Soc.* **133**, 8389 (2011).
- <sup>24</sup>M. Krasna *et al.*, *Beilstein J. Org. Chem.* **6**, 74 (2010).
- <sup>25</sup>Neeraj and K. K. Raina, *Opt. Mater.* **35**, 531 (2013).
- <sup>26</sup>O. Karaagac *et al.*, *IEEE Trans. Magn.* **46**, 3978 (2010).
- <sup>27</sup>H. Xu *et al.*, *J. Magn. Magn. Mater.* **293**, 514 (2005).
- <sup>28</sup>P. Tartaj *et al.*, *J. Phys. D: Appl. Phys.* **36**, R182 (2003).